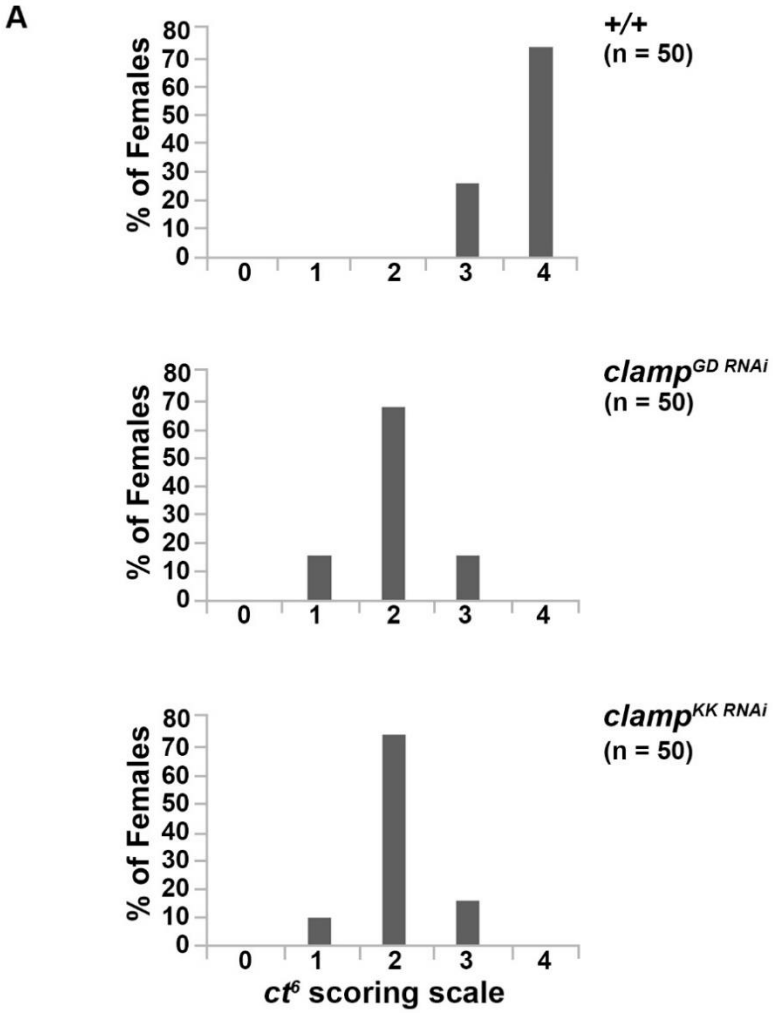

Fig. S1. Reduction of *clamp* specifically decreases *gypsy*-dependent ct^6 and y^2 enhancer blocking activities. (A) Graphical representation of ct^6 wing phenotype of female GD and KK *clamp* RNAi lines using *Ser-Gal4* driver compared to control, where "n" represents the total number of flies were scored. (B) Knockdown of *clamp* does not affect phenotype of the *gypsy*-independent ct^n allele. Wild type (left) and *clamp* RNAi lines (middle, right) driven by *Ser-Gal4* display similar wing margin phenotypes for the *gypsy*-independent ct^n loss-of function allele. (C) Example abdomens of homozygous y^2 control females (left) compared to *clamp* GD RNAi driven by *Act5C-Gal4* (right). Knockdown of *clamp* reduces enhancer blocking activity.

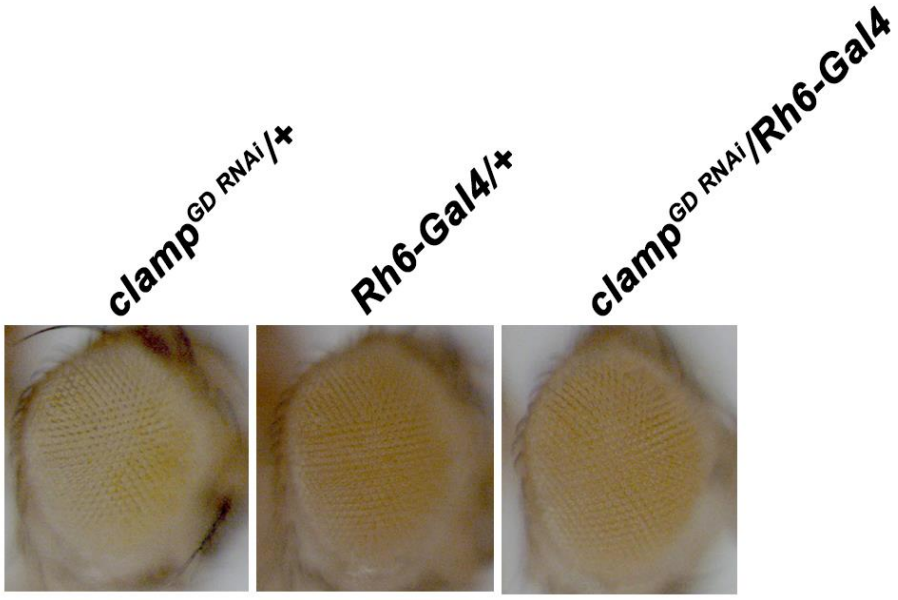

Fig. S2. *Rh6-Gal4* driver and *clamp*$^{GD\ RNAi}$ transgenes produce light background color due to mini-w^+ expression in the eye of male flies. Similarly to control flies, mini-w^+ expression of all transgenes is higher in males than females of *clamp* knockdown flies.

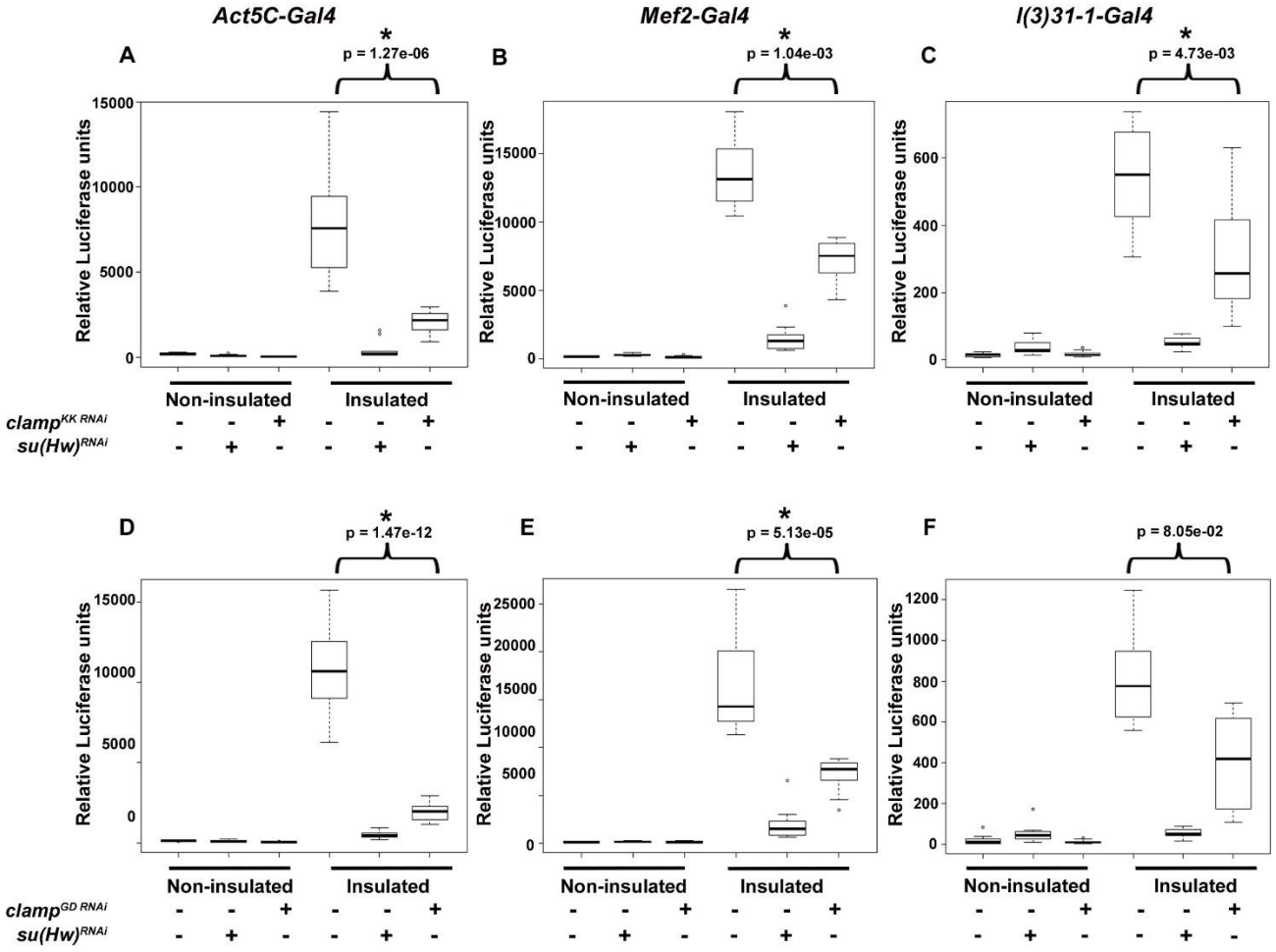

Fig. S3. Depletion of *clamp* shows decreased *gypsy*-dependent barrier activity in females in all tissues tested. (A, D) Relative luciferase activity of insulated or non-insulated female larvae of *clamp* (A) KK and (D) GD RNAi lines driven by *Act5C-Gal4*. (B, E) Relative luciferase activity of insulated or non-insulated *clamp* (B) KK and (E) GD RNAi lines driven by *Mef2-Gal4*. (C, F) Relative luciferase activity of insulated and non-insulated of *clamp* (C) KK and (F) GD RNAi lines driven by *l(3)31-1-Gal4*.

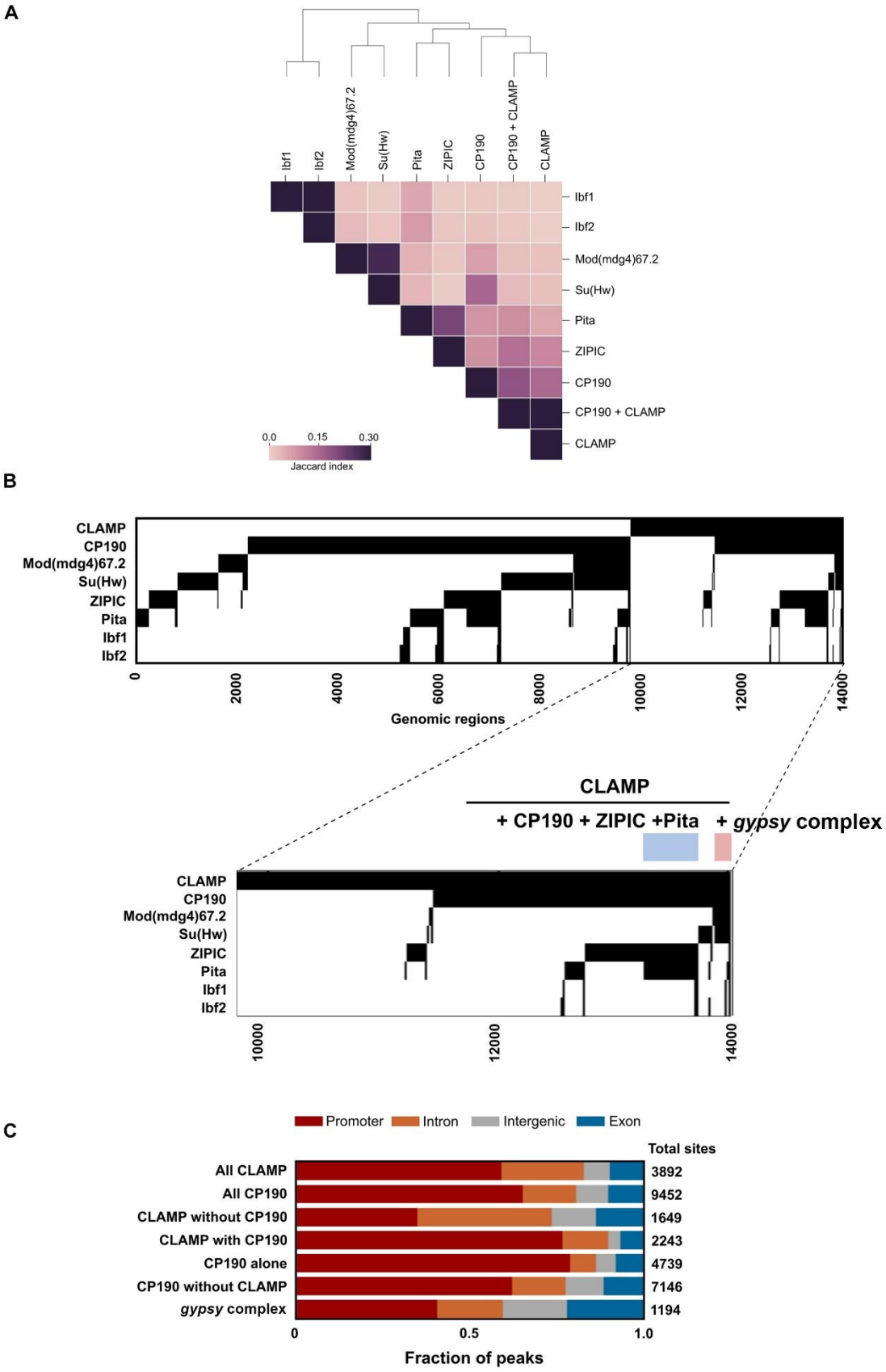

Fig. S4. Co-localization of CLAMP with Su(Hw), CP190, Mod(mdg4)67.2 and other insulator proteins. (A) Heatmap of pairwise colocalization using the Jaccard index shows the genome-wide overlap of CLAMP with *gypsy* insulator components in Kc cells and Ibf1, Ibf2, ZIPIC and Pita in S2 cells. (B) Binary heat map shows comparison of binding of CLAMP, CP190, Mod(mdg4)67.2, Su(Hw) in Kc cells and ZIPIC, Pita, Ibf1, and Ibf2 in S2 cells. A black mark in a row indicates presence of the particular factor at that genomic region. (C) Bar plot shows the occupancy of CLAMP, CP190 and *gypsy* complex binding sites at different genomic regions. 'All CLAMP' and 'All CP190' represent all CLAMP and all CP190 peaks, respectively. 'CLAMP without CP190' represents CLAMP peaks that do not overlap CP190 peaks, 'CLAMP with CP190' represents CLAMP peaks that overlap with CP190 peaks, 'CP190 alone' represents CP190 peaks that do not overlap with peaks of CLAMP or *gypsy* components, 'CP190 without CLAMP' represents CP190 peaks that do not overlap with CLAMP peaks and '*gypsy* complex' represents peaks of CP190, Su(Hw) and Mod(mdg4)67.2 that overlap together but not with CLAMP. Fraction of total peaks within a particular category is shown for each set of peaks. Number of peaks for each type of genomic region for each category is shown on right.

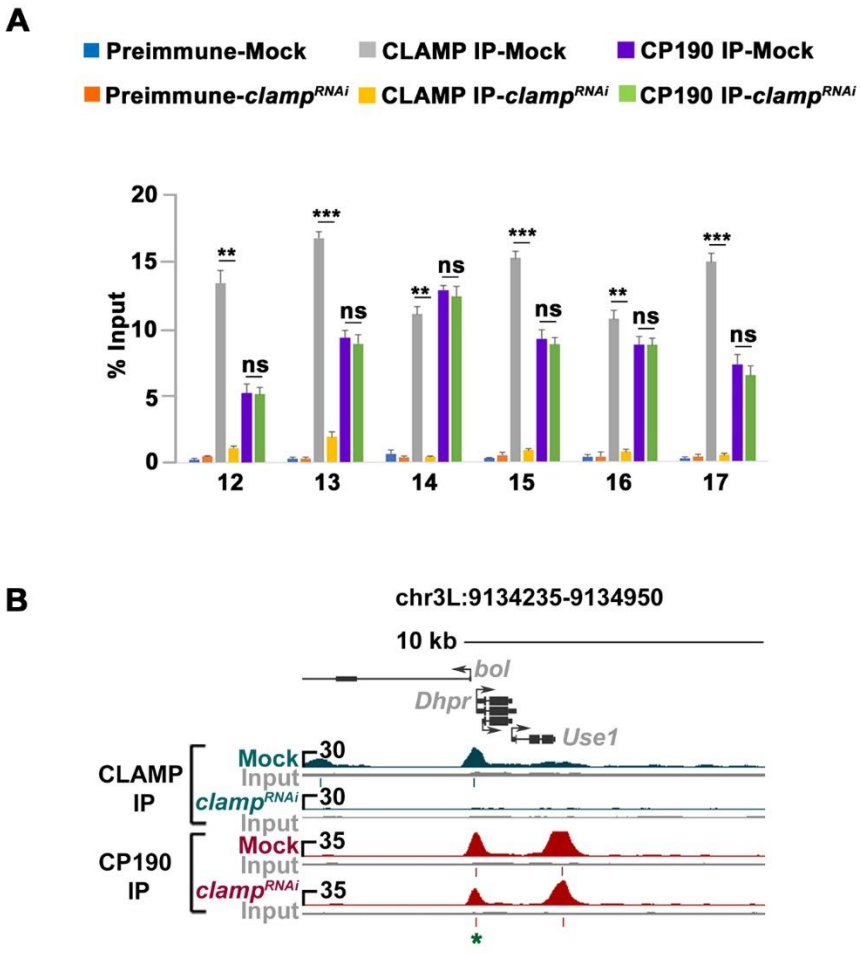

Fig. S5. Validation of CP190 association in *clamp* knockdown by directed ChIP-qPCR. (A) Validation of sites where CP190 binding remained unaffected in *clamp*^{RNAi} (sites 12-17). (B) Example screenshot for unchanged CP190 binding site is shown.

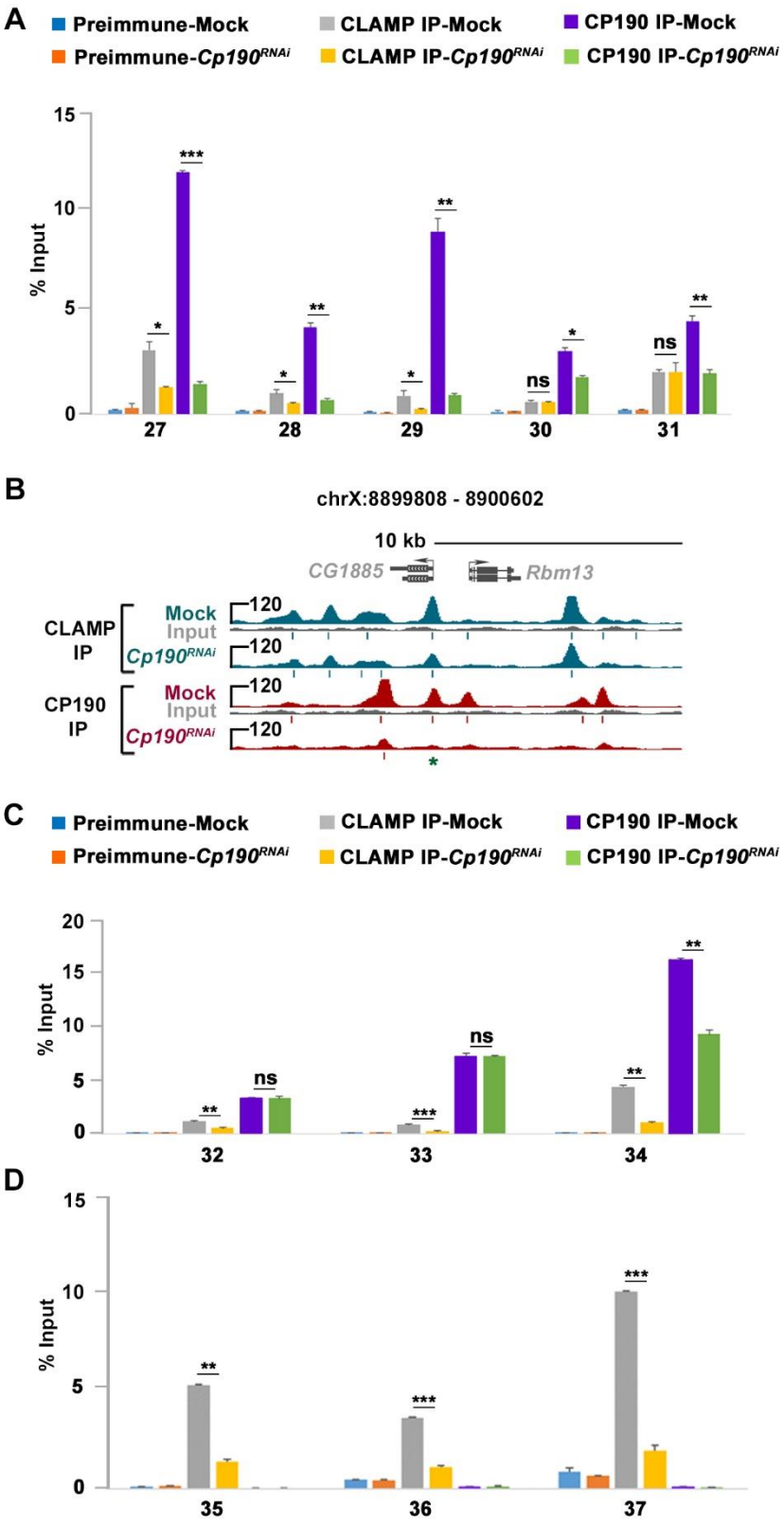

Fig. S6. Validation of CLAMP association by directed ChIP-qPCR at different genomic sites. (A) Examination of sites where CLAMP binding is reduced (sites 27-29) or remains unchanged (sites 30 and 31) in *Cp190*^{RNAi}. All five sites were called as unchanged for CLAMP by the DiffBind algorithm, indicating that loss of CLAMP was actually underrerported by this algorithm. (B) Example screenshot for unchanged CLAMP binding site at decreased CP190 site is shown. Scale for each input corresponds to the same scale for corresponding CLAMP-ChIP sample. The green color asterisk indicates the particular peak tested. (C) ChIP-qPCR of sites (sites 32 and 33) where CLAMP is decreased but CP190 remained unchanged. Another site (site 34) showed that binding of both CLAMP and CP190 are decreased. All three sites were called as unchanged for CP190 by the DiffBind algorithm, indicating that loss of CP190 was also underrerported by this algorithm. (D) Sites (sites 35-37) lacking CP190 peaks where CLAMP is decreased in depletion of CP190.

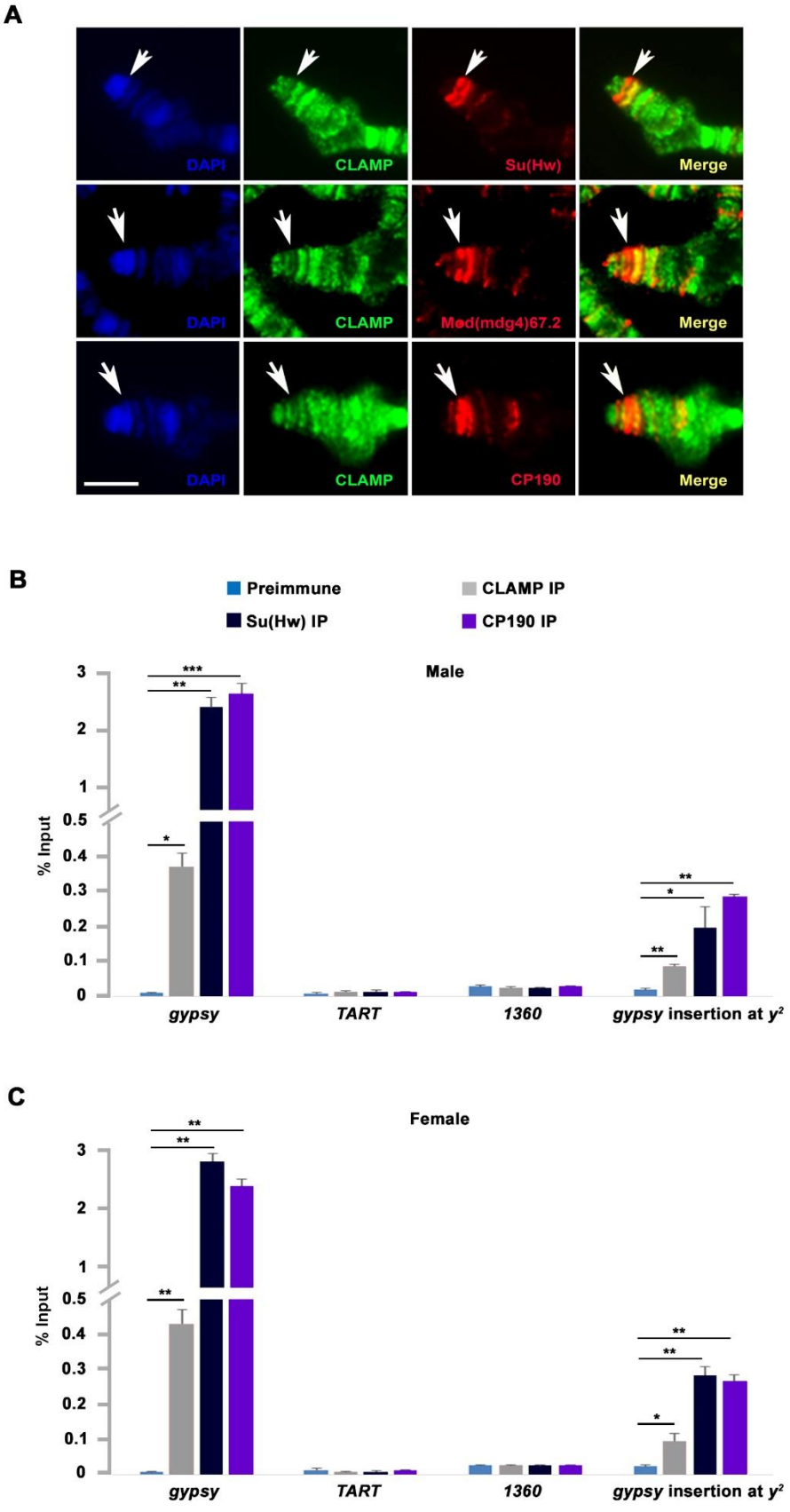

Fig. S7. Association of CLAMP and *gypsy* insulator components at the y^2 locus. (A) Immuno-co-localization of CLAMP (green) and Su(Hw) (red), Mod(mdg4)67.2 (red) or CP190 (red) are shown on polytene chromosomes. DNA is stained with DAPI (blue). White arrow indicates the y^2 locus. Scale bar equals 5 µm. ChIP-qPCR of *gypsy*, *TART*, *1360* sites and a site 585 bp upstream from the Su(Hw)-binding site in y^2 (B) male and (C) female larvae. Note that the exact Su(Hw)-binding site in y^2 could not be specifically measured due to its repetitive nature.

Supplementary tables

Table S1. Luciferase assay *p*-values for *clamp* knockdowns and all other controls using *Act5C-Gal4*, *Mef2-Gal4*, *l(3)31-1-Gal4*, and $clamp^{2}$ null using *Mef2-Gal4* in male larvae are indicated.

Click here to Download Table S1

Table S2. Luciferase assay *p*-values for *clamp* knockdowns and all other controls using *Act5C-Gal4*, *Mef2-Gal4*, *l(3)31-1-Gal4* in female larvae are indicated.

Click here to Download Table S2

Table S3. Differential binding of CP190 in $clamp^{RNAi}$ and differential binding of CLAMP in $Cp190^{RNAi}$ are verified by directed ChIP-qPCR and association of CLAMP, Su(Hw) and CP190 at *gypsy*, *TART*, *1360* and *gypsy* insertion site at y^{2} are tested by ChIP-qPCR.

Click here to Download Table S3